

Article

Impact of Distributed Generation on the Voltage Sag Performance of Transmission Systems

Pierluigi Caramia ¹ , Enrica Di Mambro ², Pietro Varilone ³  and Paola Verde ^{3,*}

¹ Department of Engineering, Università di Napoli Parthenope, 80143 Napoli, Italy; pierluigi.caramia@uniparthenope.it

² TERN Rete Italiana S.p.A, 80078 Pozzuoli (NA), Italy; enrica.dimambro@terna.it

³ Department of Electrical and Information Engineering, Università di Cassino e del Lazio Meridionale, 03043 Cassino (FR), Italy; varilone@unicas.it

* Correspondence: verde@unicas.it; Tel.: +39-077-6299-3638

Academic Editor: Frede Blaabjerg

Received: 30 May 2017; Accepted: 28 June 2017; Published: 11 July 2017

Abstract: In this paper, we analysed the growing penetration of generating units from renewable energy sources in transmission power systems. Among the possible effects of the interaction of distributed generation (DG) with transmission systems, we considered the abnormal operating conditions caused by short circuits in the transmission systems and the resulting voltage sags that occur in the network. A systematic method is presented for analysing the voltage sag behaviour of any transmission system in which large DG units are connected to the transmission system by means of High Voltage/Medium Voltage (HV/MV) stations. The method proposed for obtaining the voltage sags is the fault position method (FPM), from which we derived a graphical visualization of the during-fault voltage (DFV) matrix as a valuable tool to obtain an immediate measure of the propagation of voltage sags in the network. The results obtained were based on a portion of a real transmission system. The system that we considered is an actual portion of the Italian transmission system, and all of the quantities we used were obtained from the data of the Transmission system operator (TSO).

Keywords: power quality; voltage sag; power transmission

1. Introduction

The increasing penetration of generating units from renewable energy sources is expanding the boundaries of power system studies. Such generators typically are installed at the distribution system level, so they are driving the scientific community to deal with new problems of planning and managing distribution networks in normal and abnormal operating conditions in the presence of the so-called distributed generation (DG). The new challenges for researchers and managers involve the complete change of the distribution paradigm from passive networks with unidirectional, top-down energy flows to active networks with bi-directional energy flows [1–4].

During the planning stage, the designs of the power lines and the centralized generating units, for example, are taking advantage of the new economic and regulatory environment that allows deferring the reinforcement of the power system.

During the operation stage, the technological innovations introduced by new generating units offer new solutions for increasing the efficiency, reliability, and flexibility of the distribution service to customers, e.g., by reducing line losses and the unavailability of electricity and by meeting the customers' specific needs.

The widespread success of DG has also introduced new issues related to the impact of decentralized power generating units, consisting mainly of bi-directional power flow, the management

of complex reactive power, and the interaction of the units with the distribution network when Power Quality (PQ) disturbances occur. These problems have become more relevant due the increased awareness of the customers concerning their needs for electric service that is of good quality and reliable. The customers recognize that they are in liberalised markets, and they expect PQ levels that are close to the levels required for their own electrical loads, which tend to be technologically advanced and, thus, more vulnerable. Several studies in the relevant literature have dealt with the analysis of distribution systems in the presence of DG units, and they have focused on the benefits and the issues related to PQ [5–11]. The contributions in the literature cover a wide range of proposals; in [5,6] proper site and system indices are defined to characterize the PQ performance of systems in the presence of DG units, while in [7] the planning of DG is instead modelled on probabilistic scenarios taking into account the PQ issues that are demonstrated to be influenced by the presence of DG units. The influence of the level of penetration of the DG on the voltage-sag characteristics and propagation in the distribution network have been analysed in [8,9]. In function of the size and location of the DG and network operational practices, reference [8] shows that significant improvements in bus voltage-sag performance could be expected as a consequence of the connection of DG. In [9], the effects of mitigation of the voltage sags by converter-connected DG in the low voltage distribution networks are proved small as compared to the effects of DG on voltage sags in high voltage networks. Further papers [10,11] investigate the possibility to adequately use the DG units for mitigating the severity of the voltage sags. The comprehensive review of [10] reports several methods or schemes proposed in the literature to solve the problem of voltage sags and keep the voltage at its nominal value during the sag. Among others, in [11] two main methods are compared in terms of transient performance: the extension of the DG converter to the function of series compensator and the transfer of a vulnerable area of the network to the micro-grid operation fed by DG units.

As shown in the previous analysis of the literature, the interaction of DG units with power systems can affect the PQ levels of the systems, thereby affecting their performance due to problems that range from the variations linked to the permanent operating conditions, e.g., slow variations of voltage, harmonics and inter-harmonics, to events associated with transient operating conditions, such as voltage sags and interruptions [12]. Such interactions thoroughly have been analyzed for distribution systems, also are becoming of increasing interest for transmission systems, for which some specific aspects are particularly important. At the transmission level, in fact, the analysis must consider large DG units that are installed in medium voltage (MV) distribution networks rather than considering a huge number of small-sized DG units dispersed in several nodes. This is the typical situation of medium-to-large wind farms (with respect to power production) in MV distribution systems that are interconnected with high voltage (HV) transmission systems by HV/MV stations. The PQ aspects that affect the performance of the transmission system also are affected by the disturbances from variations to events.

Among the PQ disturbances, voltage sags caused by short circuits are of increasing interest, especially for transmission system operators (TSOs). The transmission systems provide electricity for important industrial loads that are even more vulnerable to voltage sags. The most severe effect of voltage sags is the sudden and unexpected interruption of manufacturing processes, which can cause significant economic damage to the customers fed by the TSO [13,14]. In Europe, the National Energy Regulators are activating different regulatory schemes on PQ starting from the voltage sags [15,16].

In the literature, there are several papers that have dealt with the problem of analyzing voltage sags in transmission systems [17–23]. The analyses are performed on a stochastic basis [17,18] for considering the uncertainty in several factors associated with the practical operation of a power system. Compact formulation of the equations of Fault Position Method are proposed in [19] with the aim to furnish the analytical formulation for balanced and unbalanced faults in terms of bi-dimensional vector relations and for site- and system-voltage sag indexes. Reference [20] proposes the concept of the area of vulnerability to voltage sags for evaluating relationship between sensitive loads and system voltage sag performance. Finally, in [21] the voltage sags are predicted in the entire 220 kV and 500 kV

transmission system using actual fault occurrences that took place in 2008 in the transmission system of Vietnam. All the previous papers analyzed the problem of the voltage sags in the transmission systems in which the only generation units are traditional power units. Few papers have addressed the analysis of voltage sags in transmission systems that include large DG units [22,23].

In [22], the Fault Position Method (FPM) was used to study voltage sags in the Uruguayan transmission system, which includes large wind-based generating units. The study provided an interesting characterization of the actual Uruguayan transmission system based on the concept of vulnerabilities associated with different levels of wind-based generation of electricity. Moreover, the expected behaviour of the transmission system was quantified for different load conditions and different scenarios in terms of the number of voltage sags that could cause the wind farms to be disconnected. This was obtained using the low voltage ride through characteristics of the generating units that currently require the connection of wind-based generation units to the Uruguayan electrical transmission network.

In [23], performance was analysed in terms of the voltage sags that occurred in a test power system with transmission and distribution networks. The cases were simulated in the time domain by using digSILENT PowerFactory software (V14.0, DIgSILENT GmbH, Heinrich-Hertz-Strasse 9 Gomaringen, Germany,) to analyse and compare different wind generators, different loadings on the network, and utility grids with different strengths.

In light of the information presented above, our aim in this paper was to furnish a systematic method for analysing the voltage sag behaviour of any transmission system that includes large DG units connected to the transmission system by means of HV/MV stations. In the analysis, we evaluated the impact of DG on the performance of the transmission system as a whole in short-circuit conditions and in specific busses that were selected based on their having the most vulnerable loads connected. An important feature of this paper is that the system we considered is a portion of the Italian transmission system, and all of the quantities we used were obtained from the data of the TSO.

The method proposed to obtain the voltage sags is the FPM, from which we derived a graphical visualization of the during fault voltage (DFV) matrix as a valuable tool to obtain an immediate measure of the propagation of the voltage sags in the network [24,25]. Starting from the properties of the short-circuit reactance matrices of the network, we developed the analytical expressions of the DFV already presented in [25], and we used them in this paper to adequately interpret the results obtained from the real transmission system we were studying. The voltage sag performance of the system was quantified by means of site and system indices in different operating conditions, all of which were derived from the experience of the TSO.

2. Tool for Assessing the Robustness of an Electrical Power System against Voltage Sags

The availability of tools for the analysis and prediction of the effects of voltage sags on the system's performance is of great interest. The voltage-sag frequency is, in general, so low that estimation to an acceptable degree of accuracy can be obtained only after several years of measurements. Thus, it is important to conduct theoretical analyses of the voltage sags in electrical power systems to forecast their performance.

In Italy, the on-going regulations put in place by the Italian Energy Regulator, will push the utilities toward the implementation of adequate measures to meet the quality objectives that will be imposed related to voltage sags. For the definition of the optimal solutions, there is strategic value to be obtained from the theoretical analysis of electrical power systems aimed at estimating their performance in terms of the severity of the voltage sags that occur. Voltage sags can be simulated using the FPM. This method offers a global vision of the electrical power system's response to faults because it allows the evaluation of the voltage sags in all nodes of system for faults at any bus [19]. In addition, the faults along the lines also can be simulated by introducing fictitious nodes that represent additional fault positions.

Let's refer to balanced networks in presence of three-phase faults; in this case the procedure of the FPM can be summarized as follows:

- (1) Select the position of fault f ;
- (2) Perform a short-circuit simulation;
- (3) Obtain the during-fault voltages for all electrical power system nodes;
- (4) Store the results;
- (5) Repeat steps 1 through 4 for all fault positions that must be considered (for example, positions that coincide with all nodes and have one or more points along all of the lines);
- (6) Store the during-fault voltages in the DFV matrix.

The DFV matrix is a bi-dimensional vector of voltages in which each element (i, j) represents the vector of the during-fault voltage in node i when a short circuit occurs at node j . In case of a three-phase fault, the DFV matrix, $[\bar{\mathbf{V}}_{df}]$, is given by the following relationship [19,24]:

$$[\bar{\mathbf{V}}_{df}] = [\bar{\mathbf{E}}_{pf}] - [\dot{\mathbf{Z}}_{SC}] \left(\text{diag}(\dot{\mathbf{Z}}_{SC}(1,1), \dots, \dot{\mathbf{Z}}_{SC}(n,n)) \right)^{-1} \text{diag}(\bar{\mathbf{E}}_{pf}(1), \dots, \bar{\mathbf{E}}_{pf}(n)) \quad (1)$$

where n is the number of system busbars, $[\dot{\mathbf{Z}}_{SC}]$ is the $n \times n$ nodal short circuit impedance matrix, $[\bar{\mathbf{E}}_{pf}]$ is the n vector of the pre-fault voltages, and $\left(\text{diag}([\dot{\mathbf{Z}}_{SC}]) \right)^{-1}$ is the inverse of the diagonal matrix constituted by the diagonal elements of the short circuit impedance matrix.

If the pre-fault voltages are assumed to be equal to 1 p.u., Equation (1) becomes:

$$[\bar{\mathbf{V}}_{df}] = \mathbf{J}_n - [\dot{\mathbf{Z}}_{SC}] \left(\text{diag}(\dot{\mathbf{Z}}_{SC}(1,1), \dots, \dot{\mathbf{Z}}_{SC}(n,n)) \right)^{-1} \mathbf{I}_n \quad (2)$$

where \mathbf{J}_n is a matrix full of ones such that the dimension is equal to the dimension of $[\dot{\mathbf{Z}}_{SC}]$. \mathbf{I}_n is diagonal matrix constituted by the diagonal elements equal to 1.

The method can be extended to the cases of unsymmetrical faults, as reported in [19]. The DFV matrix provides a compact view of all of the voltages registered at all of the nodes of the electrical power system. In particular, when the amplitudes of the voltages are lower than a specified value (typically 90% of the declared voltage), the nodes experience voltage sags.

The DFV matrix illustrates the properties of all sags in all nodes of the system and aggregates information on the propagation of sags throughout the network. The FPM can be used to acquire useful information, including:

- propagation of voltage sags throughout the network;
- amplitudes of the voltage sags for all nodes;
- amplitude of voltage sags caused by each node;
- nodes in which the faults are critical due to the voltage sags they cause at other nodes;
- nodes in which loads could experience the largest number of voltage sags.

A graphical color scheme was proposed to obtain immediate information on the voltage-sag performance for the entire system obtained by the FPM [19,24]. This graphical visualization allows one to immediately ascertain where changes in the external condition occurred and whether they affected the electrical power system's ability to maintain the severity of the sags at assigned levels.

Figure 1 shows a graphic visualization of the DFV matrix of a transmission electrical power system. The DFV cells are represented by colors that correspond to their values by means of the grade scale reported in the figure, i.e., blue for interruptions and white for no sag. With the exception of node 1, where there was no fault, each j th column contains the during-fault voltages for the fault at node j (affected area of node j), and each i th row contains the during-fault voltages at node i for faults in any other nodes (exposed area of node i). The graphical presentation of the DFV matrix, obtainable

for both distribution and transmission systems, is particularly effective for meshed networks, such as transmission systems.

Figure 1, as an example, shows that nodes 6 and 7 had large areas that were affected areas, and when a fault occurs in these nodes, many other nodes experience voltage sags; in fact, the sixth and seventh columns have several cells in the red range, while node 39 has the smallest exposed area. This means that this node experiences very few “light” voltage sags due to faults in other nodes. In fact, the 39th row contains only one blue cell and a few green cells.

The graphical visualization of the DFV matrix also can be used as an immediate tool to assess improvements and/or degradations of the electrical power system’s robustness in terms of the amplitudes of the voltage sags. The robustness of an electrical power system against a disturbance represents generally the intrinsic capacity to maintain assigned disturbance levels when external conditions change [24].

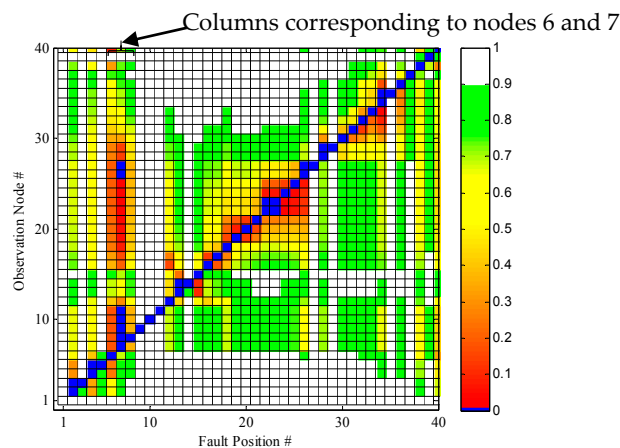


Figure 1. Graphical visualization of the DFV matrix.

Thus, the robustness of an electrical power system against voltage sags is the ability of the system to contain the severity of the voltage sags based on the structural characteristics and features of the installed components. This definition emphasizes the characteristics of the hardware, such the configuration of the network, installed generator power, and the sizes and types of the lines.

We also must ascertain the parameters required for the immediate verification of the system’s robustness. The short-circuit power at a generic bus k , S_{SC}^k , can represent an attractive global measure of the strength of the electrical system; its value, in fact, can influence the performance of the system in terms of the severity of the voltage sags.

To show this, we consider Equation (2) and write the during-fault voltage in node k due to a three-phase fault at node f :

$$\bar{V}_{k,f} = 1 - \frac{\dot{Z}_{SC}(k,f)}{\dot{Z}_{SC}(f,f)}, \quad (3)$$

where $\dot{Z}_{SC}(k,f)$ and $\dot{Z}_{SC}(f,f)$ are the (k,f) and (f,f) terms of the short-circuit matrix $[\dot{Z}_{SC}]$, respectively.

If the real parts of the terms of the short-circuit impedance matrix are neglected (as is acceptable in transmission networks while it is not true for the distribution system where X/R ratio is smaller), the short-circuit reactance matrix $[X_{SC}]$ can be considered, and relationship (3) becomes:

$$\bar{V}_{kf} = V_{kf} = 1 - \frac{X_{SC}(k,f)}{X_{SC}(f,f)} \quad (4)$$

From this equation, the DFV at node k depends on the ratio, $\frac{X_{SC}(k,f)}{X_{SC}(f,f)}$, i.e., a real quantity that ranges from zero to one. Moreover, the $[X_{SC}]$ matrix is a diagonally-dominant matrix, meaning that off-diagonal terms always are less than diagonal terms.

Given that the short circuit power at a generic node f is proportional to the quantity $1/X_{SC}(f, f)$, Equation (4) represents the link that exists between the short-circuit power level at node f and the during-fault voltage, $V_{k,f}$, at bus k when the fault occurs at node f . So, considering the short-circuit power of nodes f and k , we can compare $V_{k,f}$, given by Equation (4), with $V_{f,k}$ given by:

$$\bar{V}_{fk} = V_{fk} = 1 - \frac{X_{SC}(f, k)}{X_{SC}(k, k)} \quad (5)$$

If node k has a short-circuit power larger than that of node f , the during-fault voltage of node k for a fault in f ($V_{k,f}$) is greater than the during-fault voltage of node f for a fault in k ($V_{f,k}$). In fact, in the Equations (4) and (5), $X_{SC}(k,f) = X_{SC}(f,k)$, since the matrix $[X_{SC}]$ is symmetrical, and $X_{SC}(k,k) < X_{SC}(f,f)$.

If we compare every pair of nodes, we see that the larger the short-circuit level of a node, the less severe the voltage sags. However, the larger short-circuit level of a node, the more severe voltage sags that the node causes.

These two linkages can be viewed as the negative effect of the short-circuit power on the voltage sags caused by the node and as the positive effect of the short-circuit power on the voltage sags that the node experiences. Such properties can be easily ascertained using the graphic visualization of the DFV matrix and information on the short-circuit power levels of the nodes.

We also can examine the short-circuit reactance matrix before and after a change in the electrical power system that affects the short-circuit power of a node. Assume that $X^{new}(f, f)$ and that $V^{new}(k, f)$ are, respectively, the short-circuit reactance of node f and the during-fault voltage of a generic node k for a fault in node f after the change. The increase of the short-circuit power of the generic node f can produce voltage sags in other nodes that are more or less severe than the sags that the same node causes before that node's short-circuit power is increased. Note that the installation of a DG unit can increase the short-circuit power in the node [19]. We compare the during-fault voltage in generic node k due to the fault in f before increasing the short-circuit power of node f ($V(k, f)$) with the same quantity after the change ($V^{new}(k, f)$). Since the short-circuit reactance matrices are dominant diagonally both before the change $[X_{SC}]$ and after the change $[X_{SC}^{new}]$, we have that:

$$X_{SC}(k, f) \leq X_{SC}(f, f) \quad (6)$$

$$X_{SC}^{new}(k, f) \leq X_{SC}^{new}(f, f) \quad (7)$$

The following relationship can be verified by increasing the short-circuit power of node f :

$$X_{SC}(f, f) > X_{SC}^{new}(f, f) \quad (8)$$

Taking into account the above conditions, we have $V(k, f) \geq V^{new}(k, f)$ if:

$$1 - \frac{X_{SC}(k, f)}{X_{SC}(f, f)} \geq 1 - \frac{X_{SC}^{new}(k, f)}{X_{SC}^{new}(f, f)} \quad (9)$$

The inequality (9) can be developed as:

$$X_{SC}(k, f) \leq X_{SC}^{new}(k, f) \frac{X_{SC}(f, f)}{X_{SC}^{new}(f, f)} \text{ with } \frac{X_{SC}(f, f)}{X_{SC}^{new}(f, f)} > 1 \quad (10)$$

Relationship (10) can be expressed in terms of short-circuit power as follows:

$$X_{SC}(k, f) \leq X_{SC}^{new}(k, f) \frac{S_{SC}^{f, new}}{S_{SC}^f} \text{ with } \frac{S_{SC}^{f, new}}{S_{SC}^f} > 1 \quad (11)$$

The terms S_{SC}^f and $S_{SC}^{f, new}$ of Equation (11) are the short-circuit power at bus k before and after the change in the power system, respectively.

If condition (11) is valid, then increasing the short-circuit power in a node will have a negative effect on the performance of the other nodes in which $V^{new}(k, f) \leq V(k, f)$. If the short-circuit power of a node varies, during-fault voltages will be produced in other nodes, depending on condition given by Equation (11).

The variation of the short-circuit power of a node causes more or less severe sags in other nodes depending on conditions given by Equations (10) and (11). All of the possible conditions are summarized in Table 1. Table 1 together with the DFV matrices can support the analysis of the robustness of a distribution system in the presence of structural modifications.

Table 1. Analysis of variation due to changes in the network.

Case	Increase of S_{SC}^f	$\frac{X_{SC}^{new}(k, f)}{X_{SC}(k, f)}$	$V^{new}(k, f) - V(k, f)$
1	No	<1	>0
2	No	>1	<0 if $\frac{X^{new}(k, f)}{X(k, f)} > \frac{S_{SC}^f}{S_{SC}^{f, new}}$
3	No	>1	>0 if $\frac{X^{new}(k, f)}{X(k, f)} < \frac{S_{SC}^f}{S_{SC}^{f, new}}$
4	Yes	<1	<0 if $\frac{X^{new}(k, f)}{X(k, f)} > \frac{S_{SC}^f}{S_{SC}^{f, new}}$
5	Yes	<1	>0 if $\frac{X^{new}(k, f)}{X(k, f)} < \frac{S_{SC}^f}{S_{SC}^{f, new}}$
6	Yes	>1	<0

It is not always possible to neglect the resistances in an actual electric power system, so the considerations in Table 1 should be verified by considering the terms of the $Z_{sc}(k, f)$ matrix rather than the terms of the $X_{sc}(k, f)$ matrix, as will be shown in the numerical application in which an actual transmission system is analyzed.

3. Indices to Quantify the Severity of the Voltage Sag

The levels of the disturbances associated with voltage sags can be related to many factors that describe these disturbances, e.g., amplitude, frequency of occurrence, and duration. The available indices of voltage sags resume some of these features in a compact way so that the disturbance level can be measured by the value of the selected index. In this paper, we will refer to the site and system indices that are used most frequently in the analyses of power systems [6,26,27]. In particular, with reference to the site indices, we considered:

- The expected value of the amplitude of the voltage sag at node k ($\mu(VDA_k)$).
- The Root Mean Square (RMS) variation frequency index for retained voltage X related to site k ($RFI-X_k$).

This index indicates how often the magnitude of a voltage sag falls below a specified threshold with the value of X .

With reference to the system's indices, we considered the indices that were obtained as a weighted average of the site index, i.e.,

- the System Average Voltage Dip Amplitude (SAVDA) given by:

$$SAVDA = \frac{\sum_1^M w_k (\mu[VDA_k])}{\sum_1^M w_k} \quad (12)$$

- The System Average RMS variation Frequency Index (SARFI-X) that is given by Equation (13) for each value of X:

$$SARFI - X = \frac{\sum_1^M w_k (RFI - X_k)}{\sum_1^M w_k} \quad (13)$$

In Equations (12) and (13), w_k is the weighting factor of node k , and M is the total number of sites considered in the system in which the voltage sags arose ($M \leq N$, with N being the number of nodes in the system; in the presence of unbalanced voltage sags caused by unbalance faults, the evaluation of the SARFI-X and RFI-X indices can be performed considering the lowest magnitude for the individual phases [28]). Usually, weighting factors are introduced for all indices of the system to take into account the difference in the importance of different nodes; the weighting factors are (in most cases) assumed to be equal for all of the nodes.

It is possible to obtain the probabilistic characteristics of the sags that are needed to measure their severity by proper statistical indexes [6,21,22]. This allows derivation of the expected performance of a node or of the entire system in terms of e.g., the number of sags per year and the average amplitude of the sags. To this end, the fault voltages contained in the sag matrix must be combined with the fault rate of the system component (nodes or points along the lines) where the short circuit that is being considered originated. Let λ be the vector that contains the corresponding fault rate of each of the f fault positions:

$$\lambda = [\lambda_1, \lambda_2, \dots, \lambda_f] \quad (14)$$

The voltage sags at arbitrary node i due to the f fault positions, V_{if} , first can be grouped according to the ranges of interest (for example from 0.1 to 0.9 p.u. with the desired step). Then, as illustrated in Table 2, we compute the cumulative frequency of the voltage sags at node i , the amplitude of which falls in each range, by summing the failure rates of the fault positions that caused the sags. It is clear from (14) and from Table 1 that no closed relationships are available to calculate site and system voltage-sag indexes, so separate computations must be done. In [29], closed-form relationships were proposed that also allow the direct computation of the site and system indexes.

Table 2. Cumulative frequency of the voltage sags at node i .

Range of Amplitude of Sags (p.u.)	Frequency (Number of Sags/Year)
0.1–0.5	$\sum_j \lambda_j : V_{ij} < 0.5$
0.5–0.6	$\sum_j \lambda_j : 0.5 < V_{ij} < 0.6$
...	...
0.8–0.9	$\sum_j \lambda_j : 0.8 < V_{ij} < 0.9$

Robustness indices were introduced in [5,19,27] to synthesize the performances of the nodes in terms of affected and exposed areas. The definitions of these indices, i.e., the Affected Area Dimension Index and the Exposed Area Dimension Index are as follows:

- Affected Area Dimension index of k^{th} node (AAD_k) is the number of the network's nodes experiencing a voltage sag in presence of a fault in k^{th} node.

- Exposed Area Dimension index of k^{th} node (EAD_k) is the number of the network's nodes that, if interested by faults, produce a voltage sag in the k^{th} node.

4. Numerical Application

The impact of DG on voltage sag performance has been studied for a portion of the Italian transmission system in four different configurations. The simplified scheme and the main characteristics of the transmission system are reported in the Appendix A. We analysed the following cases:

Case A: Network without either DG or thermoelectric generation

Case B: Network with only thermoelectric generation

Case C: Network with only DG

Case D: Network with both DG and thermoelectric generation.

To model DG units, the differences in the technology of wind-based generation systems were considered. In particular, the fixed speed induction generators and doubly-fed induction generators were modeled as an asynchronous machine using transient reactance without saturation. The wind generators considered in this study are directly connected to the grid without power converter interface and with rated power equal to about 2 MW–3 MW. For these generators, the saturation is assumed negligible since the difference among unsaturated and saturated reactance values for these wind generators is slight. In fact, the manufacturer's data sheets of wind generators do not discriminate between the values of the reactance with and without saturation [30]. However, permanent magnet synchronous generators are modeled using a high value of reactance, thereby neglecting the low contributions to short-circuit currents made by generators connected to the grid with full-scale power converters.

In the network we studied, the sub-transient d-axis reactance (X_d'') was used to represent the synchronous generators of thermoelectric power plants. The resistive component in generators is negligible, and, for practical purposes, it was ignored. The reactance values were obtained from the manufacturer's data sheets.

In each case, we analysed the performance of the network in terms of the severity of the voltage sags due to the three-phase solid faults. When a voltage sag occurs, grid operators require that any generator (including wind) must have ride-through fault capability, known as "low-voltage ride through" (LVRT). The LVRT requirements stipulate that generation facilities must stay connected to the transmission system, during a fault, to support the grid stability. For this reason, the DG wind generators were assumed able to stay connected to the transmission system for all values of retained voltages.

Figure 2 shows the graphical representation of the DFV matrices for each case. A comparison of the DFV matrices makes it evident that the DG installations had a positive effect on the voltage sags in many buses of the transmission system. In fact, the connection of many DG units helped mitigate the severity of the sags. The best voltage-sag performance of the system was Case D, which had both DG and thermoelectric generation.

In the transmission system that we studied, three industrial loads (connected at nodes #68, #119, and #121) were particularly vulnerable to voltage sags due to the high sensitivity of the equipment being used in the industries' manufacturing processes. To analyse the voltage-sag performance at each industrial load's busbar during the 3-phase fault, the single corresponding i th row was extracted from the DFV matrices for all of the cases. Each i th row contains, in fact, the during-fault voltages at node i for faults in any other nodes of the system. Figures 3–5 show the rows of nodes #68, #119, and #121 for all the case studies that were considered.

From the results reported in the Figures 3–5, it is evident that the effects of the DG were beneficial for all three of the buses that were considered. For buses #68 and #121, the benefits were on "light" voltage sags, i.e., voltage sags characterised by amplitudes greater than 0.1 p.u. However, for bus

#119, the reduction of “deep” voltage sags was also registered, since some red cells became orange. As a general consideration, we can say that the severity of the voltage sags appeared to be more pronounced for nodes #119 and #121. To highlight the benefits of the DG installation on the severities of the voltage sags, the *RFI-X* and *SARFI-X* indexes were calculated with and without the presence of the DG units. For the calculation of the site and system indexes, the failure rate of each node was taken from the operating data of the transmission system. In particular, the statistical data were obtained from [31].

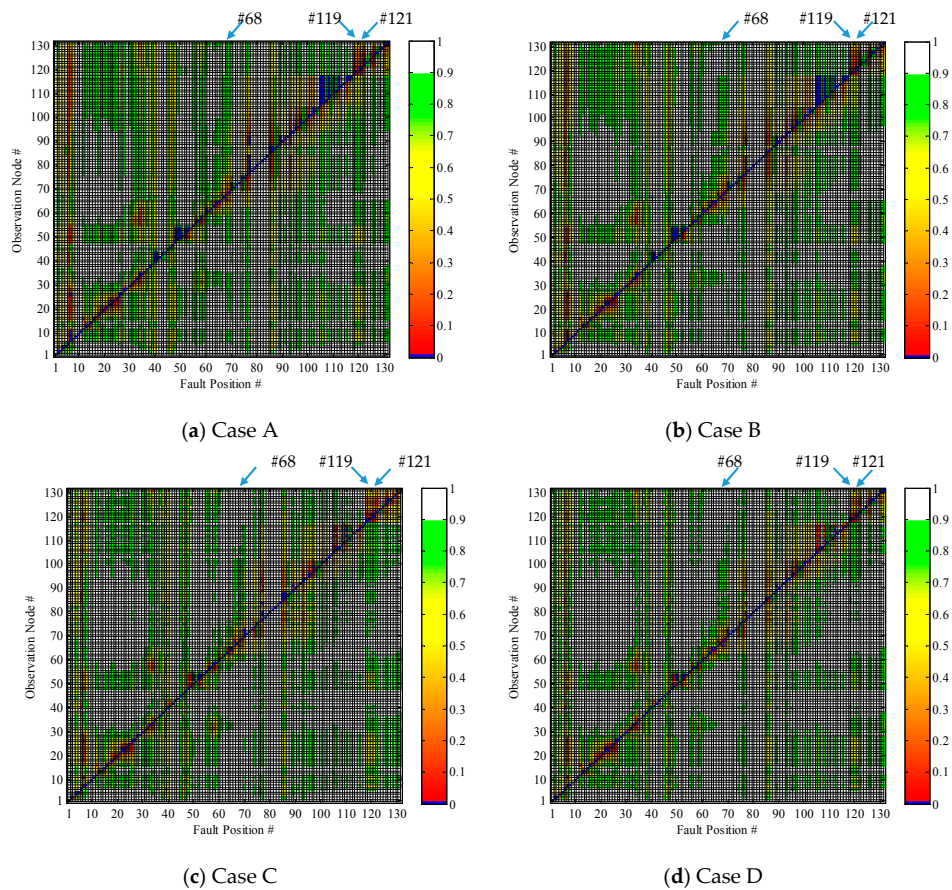


Figure 2. Graphical presentation of the DFV matrixes for all the considered cases.

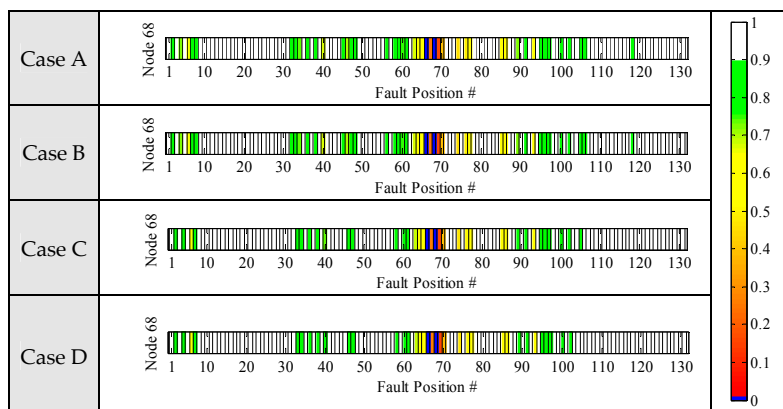


Figure 3. Graphical representation of row 68 of the DFV matrix.

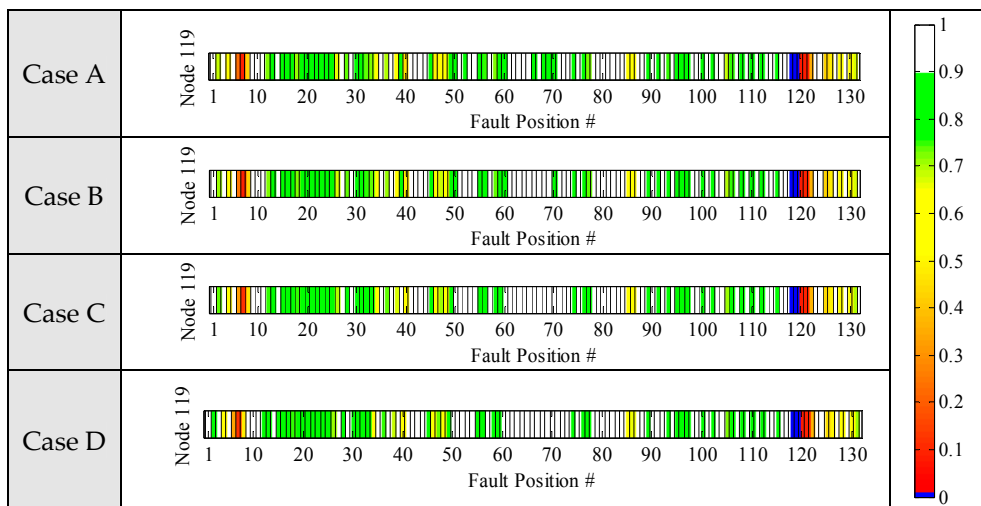


Figure 4. Graphical representation of row 119 of the DFV matrix.

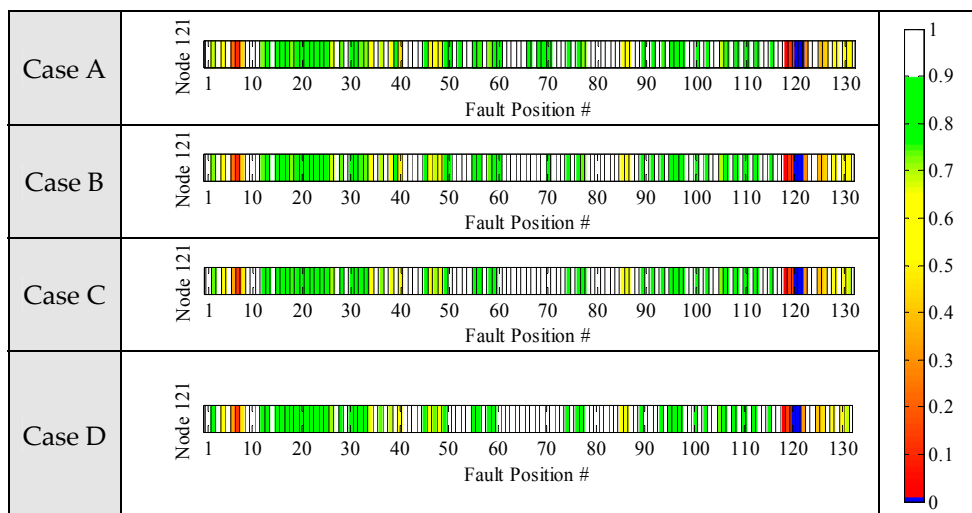


Figure 5. Graphical representation of row 121 of the DFV matrix.

Table 3 shows the system indexes for all the cases that were considered. The total number of voltage sags per year was not very different for Cases A and B, but there were significant decreases in Cases C and D due to the presence of DG.

Table 3. SARFI-X (number of sags per year) in all of the cases that were considered.

SARFI-X	Case A	Case B	Case C	Case D
SARFI-10	0.9	0.9	0.6	0.6
SARFI-20	1.7	1.6	1.0	0.9
SARFI-30	2.2	2.1	1.4	1.4
SARFI-40	2.7	2.6	2.1	2.0
SARFI-50	3.9	3.4	2.8	2.6
SARFI-60	5.1	4.8	3.9	3.6
SARFI-70	7.1	6.6	5.5	5.2
SARFI-80	11.1	10.2	8.8	8.2
SARFI-90	17.4	16.4	14.8	14.0

Tables 4–6 report the values of the *RFI-X* index for nodes #68, #119, and #121, which are particularly vulnerable to sags. From the values given in these tables, it is clear that the benefits of the DG installation are clear. In particular, the benefits are more appreciable for the most severe voltage sags. (See index from *RFI-60–RFI-90* for Case C and Case D in comparison to Case A).

Table 4. *RFI-X* (number of sags per year) in all of the cases considered for node 68.

Indexes	Case A	Case B	Case C	Case D
<i>RFI-10</i>	0.2	0.2	0.2	0.2
<i>RFI-20</i>	0.5	0.5	0.5	0.5
<i>RFI-30</i>	0.5	0.5	0.5	0.5
<i>RFI-40</i>	0.9	0.9	0.9	0.9
<i>RFI-50</i>	1.4	1.4	1.1	1.1
<i>RFI-60</i>	4.1	4.1	3.0	3.0
<i>RFI-70</i>	5.1	4.9	4.9	4.9
<i>RFI-80</i>	9.7	8.2	7.5	7.3
<i>RFI-90</i>	13.9	13.8	12.8	11.7

Table 5. *RFI-X* (number of sags per year) in all of the cases considered for node 119.

Indexes	Case A	Case B	Case C	Case D
<i>RFI-10</i>	1.9	1.9	0.6	0.6
<i>RFI-20</i>	1.9	1.9	1.9	1.9
<i>RFI-30</i>	2.4	2.4	1.9	1.9
<i>RFI-40</i>	2.6	2.6	2.6	2.6
<i>RFI-50</i>	3.8	3.5	3.3	3.2
<i>RFI-60</i>	6.0	6.0	4.6	4.3
<i>RFI-70</i>	7.7	7.5	6.6	6.6
<i>RFI-80</i>	14.1	13.4	11.9	11.7
<i>RFI-90</i>	20.9	20.4	19.1	18.5

Table 6. *RFI-X* (number of sags per year) in all of the cases considered for node 121.

Indexes	Case A	Case B	Case C	Case D
<i>RFI-10</i>	0.4	0.4	0.4	0.4
<i>RFI-20</i>	1.9	1.9	1.9	1.9
<i>RFI-30</i>	2.6	2.4	1.9	1.9
<i>RFI-40</i>	2.9	2.9	2.9	2.9
<i>RFI-50</i>	3.5	3.5	3.3	3.3
<i>RFI-60</i>	6.3	6.1	4.6	3.8
<i>RFI-70</i>	7.7	7.2	6.9	6.9
<i>RFI-80</i>	14.1	12.9	11.9	11.7
<i>RFI-90</i>	20.9	20.4	19.1	18.5

Figure 6 shows the comparison between the site (*RFI-X*) and system (*SARFI-X*) indexes. It is evident that nodes #119 and #121 had a larger number of sags than the average of the entire system.

In addition, the number of sags per year for the retained voltage 0.1 (*RFI-10*) of node 119 decreased significantly when DG was used (Case C and Case D) compared to the *RFI-10* of Case A and Case B. Figure 7 shows the plots of the exposed area dimension index, EAD_k , of nodes #68, #119, and #121 for each network configuration where thresholds were set to 90 and 30%, respectively. The EAD_k indexes of nodes #119 and #121 were greater than the EAD_k of node #68 for both thresholds. In particular, the number of the nodes contained in exposed area 90 of nodes #119 and #121 was the same for each case that was considered. However, the number of nodes contained in exposed area 30 of node #119 decreased slightly compared to the same value of node #121 in Case A. The connection of additional generation units generally caused a decreasing trend in the values, but the value of EAD_k of node #68

for the 30% threshold did not change, despite the network changes due to the different configurations that were considered.

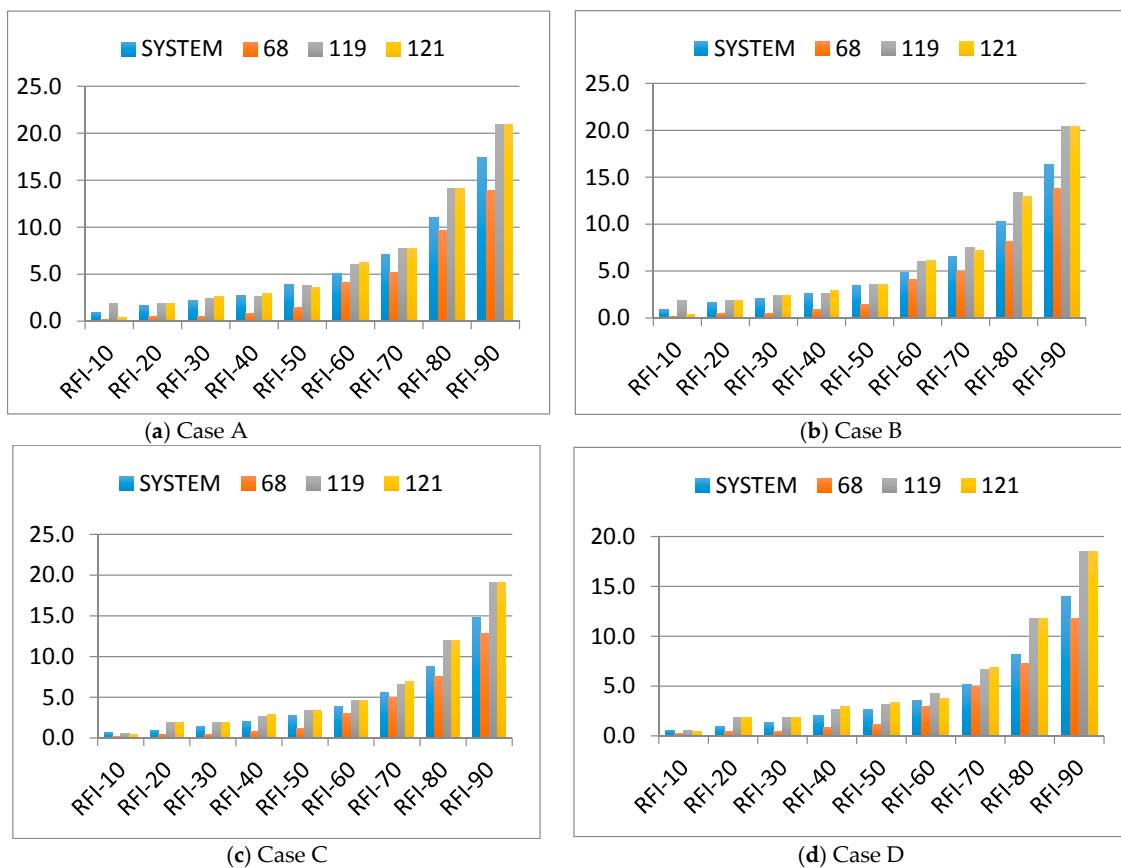


Figure 6. RFI-X and SARFI-X (number of sags/year).

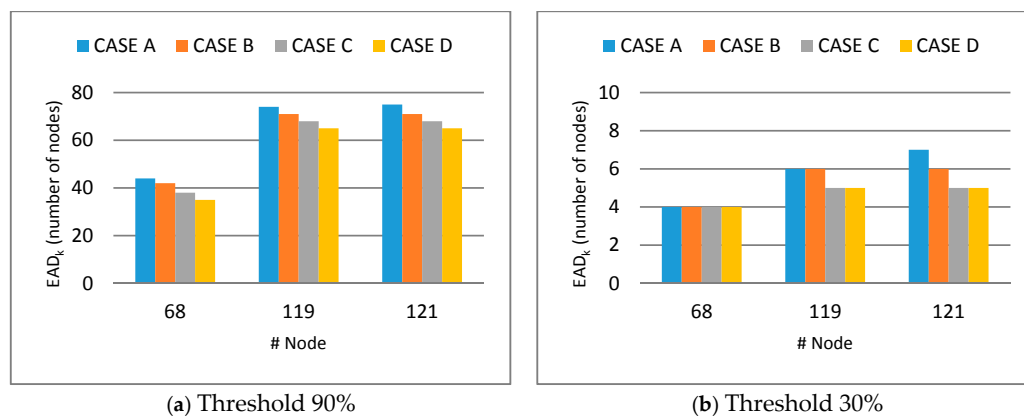


Figure 7. Exposed Area Dimension Index (number of nodes) of nodes #68, #119, and 121.

For each sensitive node, the total length (km) of the lines in exposed areas 90 and 30 was computed in every case studied. The values shown in Tables 7 and 8 were obtained by considering, for each node, the number of kilometers equal to half of the length of lines leaving the node.

The largest exposed area was in node #121 for a threshold of 90% in Case A. The number of kilometers was, in fact, about 92% of the total length of the lines of the network that we examined. However, node #68 had the smallest exposed area, with only about 38 km of lines, for threshold 30% in every configuration of the network. It was interesting to note that the exposed area 90 of node #68

decreased visibly in terms of kilometers from Case B to Case C when the DG units were connected. The connection of the DG units also caused a clear reduction of the exposed area 30 for nodes #119 and #121, as shown in Case C in Table 8.

Table 7. Total length of lines for exposed area 90.

Nodes	Case A (km)	Case B (km)	Case C (km)	Case D (km)
68	876,562	863,351	732,352	693,390
119	1,394,012	1,361,033	1,321,433	1,217,628
121	1,409,875	1,363,099	1,323,499	1,223,979

Table 8. Total length of lines for exposed area 30.

Nodes	Case A (km)	Case B (km)	Case C (km)	Case D (km)
68	37,979	37,979	37,979	37,979
119	191,147	191,147	90,082	90,082
121	197,572	191,147	90,082	90,082

Considering the installation of DG units or thermoelectric power plants as structural variations in the transmission system, the analysis of the robustness of the system performed as reported in Section 3. In particular, the variations in the short-circuit power and the short-circuit reactance matrix were examined before and after the installation of the generation units, according to the conditions of Table 1. The conditions of Table 1 were also verified for the impedance values.

The installation of the generation units in the area that we studied, as reported in Cases B, Case C, and Case D, always determined the increase in the short-circuit power if compared to Case A. In Table 1, all cases from (4) to (6) are theoretically possible.

Table 9 reports the results of the analytical analyses conducted for the nodes that were sensitive to voltage sags, i.e., #68, #119, and #121, and also for nodes #82 and #29 when both DG and thermoelectric generators were connected in the network (Case D). The faults were simulated in nodes with increased short-circuit power. For all pairs of nodes that were considered, the conditions of Table 1 were verified, and they corresponded to case (5) with the consequent improvements of the performance of the system in terms of the amplitudes of the voltage sags. The results demonstrated the validity of both the relationships for the reactance and impedance values.

Table 9. Variations due to changes in the network (Case (D)).

(k,f)	$\frac{X^{new}(k,f)}{X(k,f)}$	$\frac{Z^{new}(k,f)}{Z(k,f)}$	$\frac{S_{SC}^f}{S_{SC}^{f,new}}$	$V^{new}(k,f) - V(k,f)$
(68,34)	0.741	0.741	0.937	>0
(119,6)	0.732	0.732	0.843	>0
(121,85)	0.643	0.643	0.779	>0
(82,77)	0.355	0.357	0.789	>0
(29,28)	0.449	0.448	0.928	>0

By comparing Case C with Case B, the other conditions of Table 1 were verified, as shown in Table 10. It is interesting to note that, in node #119 for fault in #6 and also in node #121 for fault in #85, a decrease in the short-circuit power resulted in an increase in the amplitudes of the voltage sags, according to case (1) of Table 1 (the rows are identified with the grey color.)

Table 10. Variations due to changes in network Case C compared to Case B.

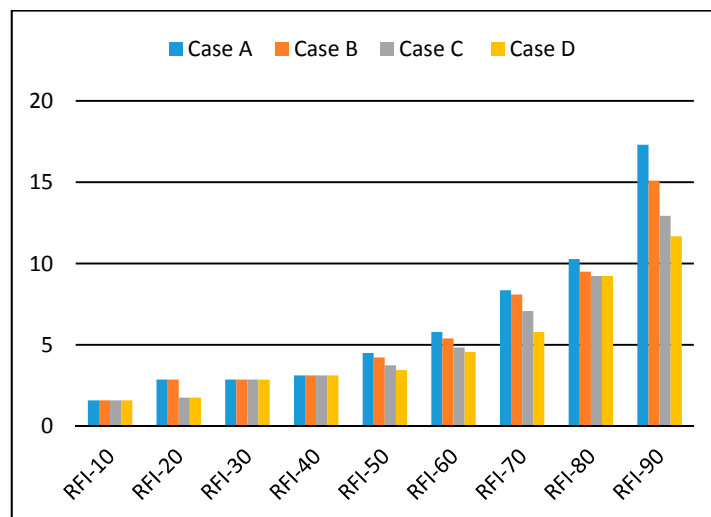
(k,f)	$\frac{X^{new}(k,f)}{X(k,f)}$	$\frac{Z^{new}(k,f)}{Z(k,f)}$	$\frac{S_{SC}^f}{S_{SC}^{f,new}}$	$V^{new}(k,f) - V(k,f)$
(68,34)	0.835	0.835	0.959	>0
(119,6)	0.926	0.926	1.030	>0
(121,85)	0.936	0.934	1.081	>0
(82,77)	0.411	0.410	0.906	>0
(29,28)	2.098	2.098	1.01	<0

We also analysed the effect of the structural variations due to the installation of a new component. In particular, as a theoretical case, we considered the connection of node #68, in which a vulnerable load was connected, to node #77, which was characterized by extensive installation of DG resulting in high short-circuit power through an ideal line in which the resistive-inductive parameters were considered to be negligible.

For this case, the *RFI-X* indexes were calculated for all of the network configurations that were analysed. These indexes are reported in Figure 8, which compares the *RFI-X* indexes obtained for the different cases.

It is evident that the number of sags per year for retained voltage from 0.5 to 0.9 p.u. of node #68 decreased in the presence of DG compared to the same *RFI-X* index of Cases A and B. In particular, for Case C, the *RFI-90* and the *RFI-20* were reduced by 25% and 38%, respectively, from the corresponding indexes of Case A.

However, the number of sags per year for retained voltages 0.1 p.u., 0.3 p.u. and 0.4 p.u. was unchanged for all of the cases.

**Figure 8.** *RFI-X* (number of sags/year) for node #68 in the theoretical case.

For node #68, Figure 9 reports a comparison of *RFI-X* indexes before and after the variation of topology, when both DG and thermoelectric generators were connected in the area that we studied (Case D). In the theoretical condition, the number of voltage decreases did not decrease for any of the retained voltages, despite the increase of short-circuit power due to the connection of node #68 to node #77.

Conditions (10) and (11) were used to better analyse the effects due to the structural modification that was considered when a fault occurred in node #68 and all generation was connected (Case D). The node chosen for observation was node #34 because it represented a 150-kV busbar of an electric

substation with high short-circuit power and it was localized not too far from the fault position. The verified conditions are reported in Table 11.

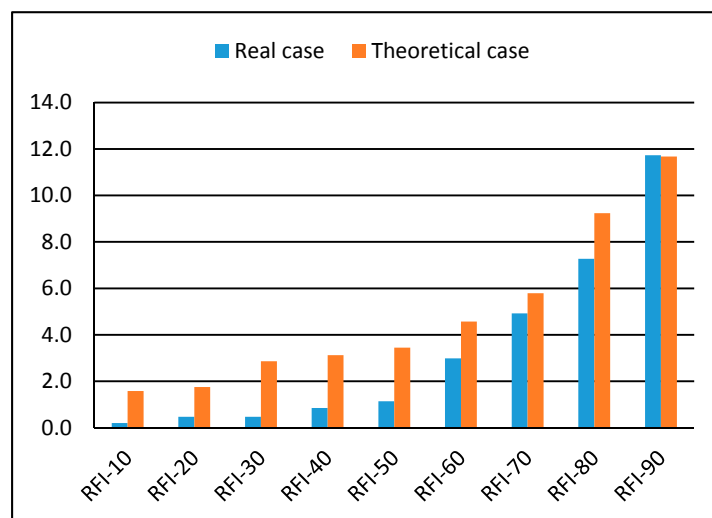


Figure 9. Comparison of RFI-X (number of sags/year) for node #68.

Table 11. Variations due to change of connection of node #68.

(k, f)	$\frac{X^{new}(k, f)}{X(k, f)}$	$\frac{Z^{new}(k, f)}{Z(k, f)}$	$\frac{S_{SC}^f}{S_{SC}^{f, new}}$	$V^{new}(k, f) - V(k, f)$
(34,68)	0.749	0.749	0.506	<0

The results showed that, in spite of the increase of short-circuit power of node #68, in the observation node there was a decrease in the amplitude of the voltage sag according to case 4 in Table 1. Indeed, the increase of short-circuit power did not result in an improvement in voltage quality in each case. The severity of the voltage sags, in fact, depended on both the variation of the short-circuit power and condition (11).

5. Conclusions

In this paper, we analysed the robustness of an electrical transmission system against voltage sags. In particular, this study provides a systematic method for analysing the behaviour of voltage sags in any transmission system in the presence of large DG units connected to the transmission system by means of HV/MV stations. The analysis was conducted by using the FPM to evaluate the impact of DG on the performance of the transmission system in short-circuit conditions in general and in specific busses selected as the busses where the most vulnerable loads were connected.

The results are presented using a graphic scheme of the matrix that contains the DFV of the nodes. The most important result was the finding that the effect of a variation of the structure of the system (connection of thermoelectric units and/or DG units) did not always improve the system's performance in terms of the severity of the voltage sags in all of the nodes, even if the short-circuit power of the nodes were increased. The results obtained for the systems we considered, which represented a real transmission system, was verified by means of FPM using the analytical expressions of the during-fault voltages.

An important feature of this paper is that the system we considered is an actual portion of the Italian transmission system, and all of the quantities we used were obtained from the data of the TSO.

Acknowledgments: This work was supported in part by the University of Napoli Parthenope in the framework of “Bando per il Sostegno alla Ricerca individuale per il triennio 2015–2017. The authors also wish to thank TERNA S.p.A for sharing their data with us during the course of this research.

Author Contributions: The authors contributed equally to this work.

Conflicts of Interest: The authors declare no conflict of interest.

Abbreviations

AAD_k	Affected Area Dimension index of k^{th} node
EAD_k	Exposed Area Dimension index of k^{th} node
DG	Distributed generation
DFV	During-fault voltage
FPM	Fault position method
PQ	Power Quality
$RFI-X_k$	RMS variation frequency index for retained voltage X related to site k
SARFI-X	system average RMS variation frequency index
SAVDA	system average voltage sag amplitude
TSO	Transmission system operator

Appendix A

The network used in this study was a simplified model that represents a part of the National Transmission System of Italy (380 kV and 150 kV) as of December 2015. The scheme of the transmission system is reported in Figure A1 (data for the study were obtained from TERN, the Italian TSO). The system consists of 131 buses and 89 overhead lines and underground cables with a total length of 1534 km. It includes five electric substations that interconnect 380 and 150-kV systems. In particular, buses 1, 2, 4, 6, 38, 39, 40, 46, 47, and 85 form part of the 380-kV transmission level. The generator busbars of the network are the interconnection nodes (busbars #1, #15, #36, #37, #39, #45, #47, and #67).

It is an active network that includes three large, thermoelectric power plants (971 MVA) and 41 renewable energy source generators. Wind-based power represents 97% of the total renewable power installed (1388 MVA) in the network we studied. The remaining 3% consists of photovoltaic systems that are not considered in this paper. The DG power plants are connected at the distribution level.

Three industrial loads (located at buses #68, #119, and #121) were identified as particularly sensitive to voltage sags in the area that we analysed.

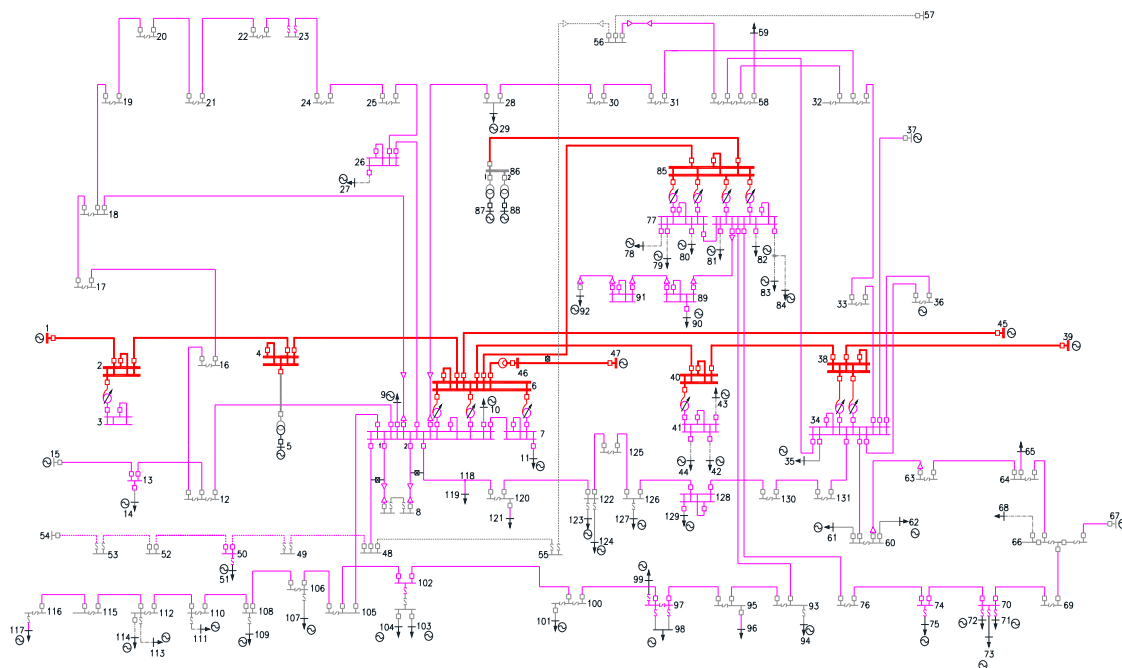


Figure A1. The transmission system.

References

1. Borbely, M.; Kreider, J.F. *Distributed Generation. The Power Paradigm for the New Millennium*; CRC Press: Boca Raton, FL, USA, 2001; ISBN 0-8493-0074-6.
2. Pepermans, G.; Driesen, J.; Haeseldonckx, D.; Belmans, R.; D'haeseleer, W. Distributed generation: Definition, benefits and issues. *Energy Policy* **2005**, *33*, 787–798. [[CrossRef](#)]
3. Jenkins, N.; Allan, R.; Crossley, P.; Kirschen, D.; Strbac, G. *Embedded Generation*; Institution of Electrical Engineers: London, UK, 2000.
4. McDermott, T.E.; Dugan, R.C. PQ, reliability and DG. *IEEE Ind. Appl. Mag.* **2003**, *9*, 17–23. [[CrossRef](#)]
5. Caramia, P.; Carpinelli, G.; Verde, P. *Power Quality Indices in Liberalized Markets*; Wiley: Chichester, UK, 2009; ISBN 978-0-470-03395-1.
6. Bracale, A.; Caramia, P.; Carpinelli, G.; Russo, A.; Verde, P. Site and System Indices for Power-Quality Characterization of Distribution Networks. *IEEE Trans. Power Deliv.* **2011**, *26*, 1304–1316. [[CrossRef](#)]
7. Carpinelli, G.; Celli, G.; Pilo, F.; Russo, A. Embedded generation planning under uncertainty including power quality issues. *Eur. Trans. Electr. Power* **2003**, *13*, 381–389. [[CrossRef](#)]
8. Milanovic, J.V.; Ali, H.; Aung, M.T. Influence of distributed wind generation and load composition on voltage sags. *IET Gener. Transm. Distrib.* **2007**, *1*, 13–22. [[CrossRef](#)]
9. Renders, B.; de Gussemè, K.; Ryckaert, W.R.; Stockman, K.; Vandeveld, L.; Bollen, M.H.J. Distributed Generation for Mitigating Voltage Dips in Low-Voltage Distribution Grids. *IEEE Trans. Power Deliv.* **2008**, *23*, 1581–1588. [[CrossRef](#)]
10. Ipinimo, O.; Chowdhury, S.; Chowdhury, S.P. Voltage Dip Mitigation with DG Integration: A Comprehensive Review. In Proceedings of the Joint International Conference on Power Electronics, Drives and Energy Systems (PEDES) & 2010 Power India, New Delhi, India, 20–23 December 2010.
11. Macken, K.J.P.; Bollen, M.H.J.; Belmans, R.J.M. Mitigation of voltage dips through distributed generation systems. *IEEE Trans. Ind. Appl.* **2004**, *40*, 1686–1693. [[CrossRef](#)]
12. European Committee for Electrotechnical Standardization. *Voltage Characteristics of Electricity Supplied by Public Distribution Networks*; EN50160; European Committee for Electrotechnical Standardization: Brussels, Belgium, 2011.
13. Joint Working Group Cigre/Cired C4.110. *Voltage Dip Immunity of Equipment and Installations*; Report 412; Cigré: Rio de Janeiro, Brasil, 2010.
14. Di Fazio, A.R.; Duraccio, V.; Varilone, P.; Verde, P. Voltage sags in the automotive industry: Analysis and solutions. *Electr. Power Syst. Res.* **2014**, *110*, 25–30. [[CrossRef](#)]
15. European Parliament, Council of the European Union. *Directive 2009/72/EC of the European Parliament and of the Council of 13 July 2009 Concerning Common Rules for the Internal Market in Electricity and Repealing Directive 2003/54/EC (“3rd Package”)*; European Parliament, Council of the European Union: Brussels, Belgium, 2009.
16. Council of European Energy Regulators (CEER), 5th CEER Benchmarking Report on the Quality of Electricity Supply, Brussels, Belgium. 2011. Available online: http://www.ceer.eu/portal/page/portal/EER_HOME/EER_PUBLICATIONS/CEER_PAPERS/Electricity/Tab/CEER_Benchmarking_Report.pdf (accessed on 1 April 2011).
17. Faried, S.O.; Billinton, R.; Aboreshaid, S. Stochastic Evaluation of Voltage Sag and Unbalance in Transmission Systems. *IEEE Trans. Power Deliv.* **2005**, *20*, 2631–2637. [[CrossRef](#)]
18. Park, C.-H.; Jang, G. Stochastic estimation of voltage sags in a large meshed network. *IEEE Trans. Power Deliv.* **2007**, *22*, 1655–1664. [[CrossRef](#)]
19. Carpinelli, G.; Caramia, P.; di Perna, C.; Varilone, P.; Verde, P. Complete matrix formulation of fault-position method for voltage-dip characterization. *IET Gener. Transm. Distrib.* **2007**, *1*, 56–64. [[CrossRef](#)]
20. Park, C.H.; Jang, G. Systematic method to identify an area of vulnerability to voltage sags. *IEEE Trans. Power Deliv.* **2017**, *32*, 1583–1591. [[CrossRef](#)]
21. Khanh, P.Q.; Phuc, N.H. Prediction of voltage sag in the transmission system of Vietnam, A case study. In Proceedings of the IEEE/PES Power Systems Conference and Exposition, Phoenix, AZ, USA, 20–23 March 2011.
22. Afonso, J.I.; Giusto, M.A.A. Voltage dip analysis in the Uruguayan transmission network in high penetration wind generation scenarios. In Proceedings of the 2012 Sixth IEEE/PES Transmission and Distribution: Latin America Conference and Exposition (T&D-LA), Montevideo, Uruguay, 3–5 September 2012.

23. Sekhoto, P.; Ipinnimo, O.; Chowdhury, S. Voltage dip analysis of electricity networks on wind energy integration. In Proceedings of the 48th International Universities Power Engineering Conference (UPEC), Dublin, Ireland, 2–5 September 2013.
24. Caramia, P.; Carpinelli, G.; di Perna, C.; Varilone, P. Methods for assessing the robustness of electrical power systems against voltage dips. *IEEE Trans. Power Deliv.* **2009**, *24*, 43–51.
25. Bracale, A.; Caramia, P.; Varilone, P.; Vitale, L.; Verde, P. *On the Evaluation of Voltage Dip Performance of Micro-Grids*; CIGRE (Conseil International des Grands Réseaux Électriques): Bologna, Italy, 2011; ISBN 9782858731657.
26. *Recommended Practice for Establishment of Voltage Sag Indices (Draft 6)*; IEEE P1564/d6; IEEE Power Engineering Society: New York, NY, USA, 2004.
27. Di Perna, C.; Olguin, G.; Verde, P.; Bollen, M.H.J. On probabilistic system indices for voltage dips. In Proceedings of the 2004 International Conference on Probabilistic Methods Applied to Power Systems, Ames, IA, USA, 12–16 September 2004.
28. Institute of Electrical and Electronic Engineers. *IEEE Guide for Voltage Sag Indices*; IEEE: Piscataway, NJ, USA, 2014; ISBN 978-0-7381-9138-6.
29. *Power Quality Indices and Objectives*; Final WG Report 261; Joint Working Group, CIGRE C4.07/Cired (formerly Cigre WG 36.07): Rio de Janeiro, Brazil, 2004.
30. *Manufacturer's Generator Data Sheet VESTAS*; Item n. 944904; Vestas: Aarhus, Denmark, April 2003.
31. Monitoring and Business Intelligence (MBI). *Terna's Operation and Maintenance Support System*; Monitoring and Business Intelligence (MBI): Roma, Italy, 2010.



© 2017 by the authors. Licensee MDPI, Basel, Switzerland. This article is an open access article distributed under the terms and conditions of the Creative Commons Attribution (CC BY) license (<http://creativecommons.org/licenses/by/4.0/>).